PHOTON COUNTING CHIRPED AM LADAR: CONCEPT, SIMULATION, AND EXPERIMENTAL RESULTS

Brian Redman, William Ruff, and Mark Giza
Army Research Laboratory, 2800 Powder Mill Road, Adelphi, MD 20783

ABSTRACT

The operating principles and experimental results for the Army Research Laboratory's (ARL's) patented chirped amplitude modulation (AM) ladar using linear response detectors have been presented and published previously, and will be briefly summarized here (Stann, et. al., 1996). In ARL's current prototypes using unity gain detectors, amplifier noise limits the receiver sensitivity. This noise is well above the signal shot noise limit. We are developing a method using Geiger-mode avalanche photodiode (Gm-APD) photon counting detectors in the chirped AM ladar receiver to yield sensitivities approaching the shot noise limit. Such sensitivities represent about four orders-of-magnitude improvement over the sensitivities of the currently used unity-gain, opto-electronic mixing (OEM) metal-semiconductor-metal (MSM) detectors.

The sensitivity improvement demonstrated by the photon counting chirped AM ladar experiments may enable very compact, low power, eye-safe, and/or long range ladars with low cost, low bandwidth readout integrated circuits (ROICs).

1. INTRODUCTION

Although for a single photon detection the output voltage of a Gm-APD single photon counting module (SPCM) is a count pulse of constant amplitude that is not proportional to the light power, the AM waveform can be measured since the mean arrival rate of photons at the detector is proportional to the light power even though individual photon arrivals are randomly distributed (Drain, 1980). Thus, the mean photon arrival rate, and therefore, the photon count rate output by a Gm-APD SPCM, will be modulated by an amplitude modulation of the light power. This process is akin to the use of pulse position modulation (PPM) to convert analog amplitude signals to digital data streams in digital telecommunications systems.

In ARL's patented chirped AM ladar, the transmitted laser power is amplitude modulated with a sinusoid for which the frequency is changed linearly with time from a low (high) frequency to a high (low) frequency, corresponding to an up (down) chirped AM waveform. The chirped AM waveform is preserved, with a round-trip time delay, for the laser light backscattered from a target into the ladar receiver so that the mean photon arrival rates at the receiver are modulated with the time shifted chirp waveform. The range to the target is recovered in the same way as for the chirped AM ladar with linear response mode detectors.

In this paper, we summarize the theory of operation for chirped AM ladars with linear response detectors, and discuss the theory of operation using SPCMs. Then we present the calculation of the signal-to-noise ratio (SNR) for the photon counting chirped AM ladar based on the theory of operation. Next, we present the results of computer and electronic simulations based on the theory of operation. Finally, we present the results of optical experiments demonstrating the operation of the photon counting chirped AM ladar.

2. THEORY

2.1 Chirped AM Ladar Theory

The chirped AM waveform is a variation of the familiar frequency modulation-continuous wave (FM-CW) waveform used in radar and coherent ladar. For chirped AM, however, the frequency modulation is applied to the frequency of an amplitude modulation of the laser output power rather than being applied directly to the frequency of the laser light (i.e., to the frequency of the electromagnetic wave) as for coherent ladars and for FM-CW radars. In this way, chirped AM ladars can use optical direct detection instead of needing to employ an optical local oscillator (LO) as required for coherent ladars. For the chirped AM ladar, the LO is a radio-frequency (RF) electrical signal as used in FM-CW radars. ARL's chirped AM ladar uses a sawtooth FM-CW waveform for which the frequency of the amplitude modulation is changed linearly with time from a low (high) frequency to a high (low) frequency, corresponding to an up (down) chirped AM waveform, as depicted in Figure 1. A detailed explanation of the signal processing used to measure the target velocity and range can be found in most books that discuss radar theory. Here, we briefly discuss some of the basic operating theory for clarity.

The transmitted chirp waveform, which is also used as the electronic RF LO waveform, is shown in the frequency versus time diagram of Figure 1 as a solid line, with the dotted line representing the chirp waveform received from the target. The received chirp waveform is nearly identical to the transmitted waveform except that

Report Documentation Page

1. REPORT DATE **01 NOV 2006**	2. REPORT TYPE **N/A**	3. DATES COVERED **-**	
4. TITLE AND SUBTITLE **Photon Counting Chirped Am Ladar: Concept, Simulation, And Experimental Results**		5a. CONTRACT NUMBER	
		5b. GRANT NUMBER	
		5c. PROGRAM ELEMENT NUMBER	
6. AUTHOR(S)		5d. PROJECT NUMBER	
		5e. TASK NUMBER	
		5f. WORK UNIT NUMBER	
7. PERFORMING ORGANIZATION NAME(S) AND ADDRESS(ES) **Center for Theoretical Studies of Physical Systems and, Department of Computer and Information Science Clark Atlanta University Adelphi, MD 20783 Atlanta, GA 30314**		8. PERFORMING ORGANIZATION REPORT NUMBER	
9. SPONSORING/MONITORING AGENCY NAME(S) AND ADDRESS(ES)		10. SPONSOR/MONITOR'S ACRONYM(S)	
		11. SPONSOR/MONITOR'S REPORT NUMBER(S)	
12. DISTRIBUTION/AVAILABILITY STATEMENT **Approved for public release, distribution unlimited**			
13. SUPPLEMENTARY NOTES **See also ADM002075.**			
14. ABSTRACT			
15. SUBJECT TERMS			

16. SECURITY CLASSIFICATION OF:			17. LIMITATION OF ABSTRACT **UU**	18. NUMBER OF PAGES **8**	19a. NAME OF RESPONSIBLE PERSON
a. REPORT **unclassified**	b. ABSTRACT **unclassified**	c. THIS PAGE **unclassified**			

it is delayed with respect to the transmitted waveform by the round-trip time between the ladar and the target, i.e., $\tau = 2R/c$, where R is the target range and c is the speed of light, and the received waveform is shifted in frequency due to the Doppler frequency shift induced by the target motion along the ladar's line-of-sight.

As seen from the diagram in Figure 1, at any instant of time, there is a difference in frequency between the transmitted waveform and the received waveform. If the transmitted waveform is used as an LO and mixed with the received waveform, the product will contain a beat at the difference frequency referred to as the intermediate frequency (IF) waveform.
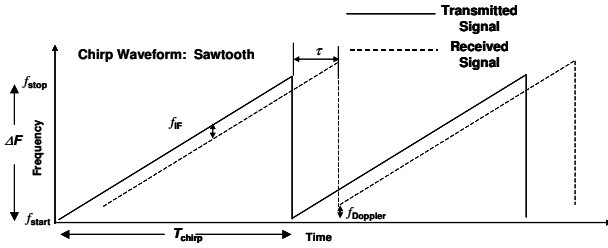

Figure 1. Transmitted and received signal for an FM-CW or chirped AM system with a sawtooth up-chirp.

For the stationary target case, the IF is given by

$$f_{IF} = \tau \frac{\Delta F}{T_{chirp}} = \frac{2R\Delta F}{cT_{chirp}} \ , \tag{1}$$

where ΔF = the chirp bandwidth = f_{stop} - $f_{start,}$ and T_{chirp} = chirp period/duration.

Solving equation (1) for R expresses the range as a function of the IF, f_{IF}. Taking the magnitude of the fast Fourier transform (FFT) of this signal over a chirp period allows the signal's IF, or equivalently, the target range to be easily measured since the magnitude spectrum contains a peak at the IF. The frequency resolution of this measurement is equal to $1/T_{chirp}$ which corresponds to a range resolution of $\Delta R = c/2\Delta F$. Each frequency cell in the FFT is also referred to as a range cell.

For the case of a moving target, the IF will be shifted in frequency by the average Doppler frequency shift over the chirp waveform, so that

$$f_{IF} = \tau \frac{\Delta F}{T_{chirp}} \pm f_{Doppler},$$

where $f_{Doppler} = \frac{2vf_{center}}{c}$, \tag{2}

$$f_{center} = f_{start} + \Delta F/2$$
= the center frequency,
c = the speed of light, and
v = the target LOS velocity

If the IF signal is measured only over a single chirp, the measured frequency will be the result of both the unknown range and unknown Doppler frequency shift. This single chirp measurement cannot separately determine these two frequencies. Since the complex phasor rotates at the Doppler frequency, the amount of rotation, which corresponds to a shift in the starting phase of the IF waveform from chirp-to-chirp, can be sampled from chirp-to-chirp using the sawtooth waveform. In this case, the chirp rate must be several times greater than the Doppler frequency shift to adequately sample the Doppler frequency shift. Then, simply taking a second FFT at each range cell (resulting from the first FFT over each chirp) across a number of repeated chirps, maps the data into a Range-Doppler space with two frequency axes, one corresponding to range and one corresponding to Doppler frequency shift. Using this technique, the Doppler frequency shift measurement resolution is limited by the duration of the measurement over multiple (N) chirps, i.e., $1/T_{Doppler} = 1/NT_{chirp}$.

2.2 Photon Counting Chirped AM Theory

As shown in Figure 2, intensity/power modulation of light produces a corresponding modulation in the photon average temporal intervals, which produces the corresponding modulation in the photon mean arrival rates at a receiver (Drain, 1980.). Thus, the chirped AM waveform that modulates the transmitted laser power also modulates the photon mean arrival rates at the receiver with a delay corresponding to the round-trip time between the transceiver and the target. This forms the basis for the photon counting chirped AM ladar technique.
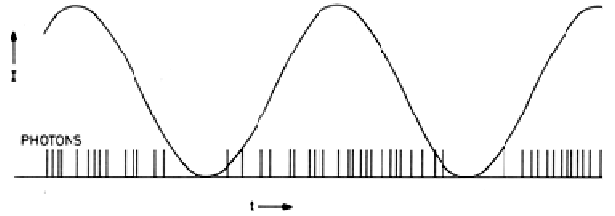

Figure 2. Random photon arrival pattern for the fully modulated sinusoidal intensity variation shown (Drain, 1980).

The output voltage of a Gm-APD SPCM is a constant amplitude count pulse for a photon detection, and is not proportional to the incident light power. In most cases, the count pulse has a duration equal to the quenching time of the quenching circuit following the Gm-APD, and this usually dominates the Gm-APD dead time, which is the sum of the quenching time and the reset time. Typically, the dead time can be from tens of nanoseconds to several microseconds, although shorter dead times are attainable with specially designed quenching circuits. The rise time of the count pulse,

however, is typically sub-nanosecond. The count pulse rise time sets the upper limit of the photon counting receiver bandwidth, and therefore, sets the minimum achievable timing/range resolution. The inverse of the dead time sets the upper limit on the photon arrival rate since subsequent photons incident on the receiver in times less than the dead time from the arrival of the previous photon will not produce a count pulse. This results in errors in the measurement of the arrival rate modulation.

As shown in the block diagram of the photon counting chirped AM ladar with post-detection mixing in Figure 3, the Gm-APD's output count pulse edge triggers a short pulse generator to output a short pulse of a duration that is less than or equal to $1/(4 \cdot f_{chirp\_max})$ where f_{chirp_max} = the maximum frequency in the chirp waveform.
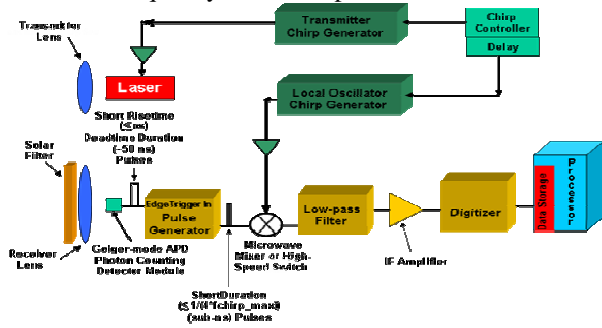

Figure 3. Photon Counting Chirped AM Ladar with Post-detection Mixing Block Diagram.

The resulting arrival rate modulated short pulses are mixed with a radio-frequency (RF) local oscillator (LO) having the same chirp waveform as the transmitter to produce a series of random pulses with mean arrival rates modulated by the product of the LO and received light modulation waveforms, i.e., the intermediate frequency (IF) waveform. Low-pass (or bandpass) filtering the mixer output yields a sinusoid with a frequency proportional to the round-trip time between the ladar transceiver and the target. Digitizing the IF waveform and taking the magnitude of the fast Fourier transform (FFT) of the data produces the IF magnitude spectrum, for which there is a peak at a frequency proportional to the round-trip time with an amplitude proportional to the mean return signal.

In the alternate configuration shown in Figure 4, the LO is applied to gate the excess bias voltage above and below the Gm-APD's breakdown bias voltage to provide opto-electronic mixing (OEM) with a square wave LO at the detector. In this OEM configuration, the detector's minimum gate duration must be less than one-half of the reciprocal of the highest frequency in the chirp waveform, and the maximum gate repetition rate must be at least equal to the highest frequency in the chirp waveform. In the OEM configuration, the output of the SPCM will have an envelope that is modulated with the

IF waveform which is recovered by low-pass or bandpass filtering. As usual, digitizing the IF waveform and taking the magnitude of the FFT of the data produces the IF magnitude spectrum, for which there is a peak at a frequency proportional to the round-trip time with an amplitude proportional to the mean return signal.
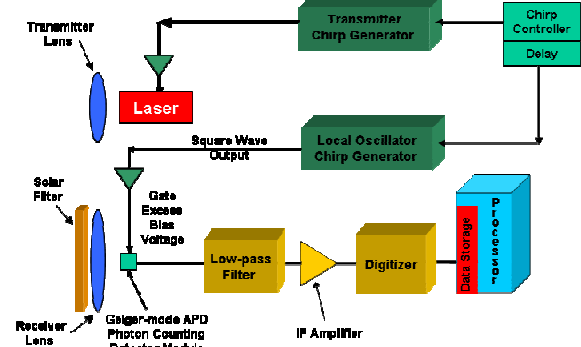

Figure 4. Photon Counting Chirped AM Ladar with Opto-Electronic Mixing (OEM) Block Diagram.

2.3 Signal-to-Noise Ratio for Photon Counting Chirped AM Ladar

It is important to note the possible polarities of the modulation waveforms for different ladar configurations because the modulation waveform polarities will affect the achievable peak signal to mean square noise electrical power SNR. For the traditional FM-CW waveform applied to the electromagnetic wave in radar and coherent ladar, the transmitted/received signal modulation waveform is two-sided (i.e., alternates between positive and negative polarities, aka bipolar), the LO modulation waveform is two-sided (bipolar), and the resulting IF waveform is two-sided (bipolar). For a given number of photons in a measurement, the case for which both the signal and LO are bipolar results in the maximum SNR.

In the case of the chirped AM waveform, the signal modulation is one-sided (i.e., single polarity aka unipolar) since negative optical power is not possible. This results in a factor of two (3 dB) loss in the electrical power SNR for 100% modulation depth compared to the radar or coherent ladar configuration for the same number of photons in a measurement. For post-detection mixing with a balanced mixer, the LO waveform is two-sided (bipolar), as is the output IF waveform, so there is no further loss in SNR in this configuration.

For the OEM mixing configuration, the LO waveform and the output IF waveform are both one-sided (unipolar). In this case, there is an additional factor of 4 (6 dB) loss in electrical power SNR compared to the bipolar case (Wozencraft, 1965). Part of the loss (3 dB) goes into the constant (i.e., DC) component produced by

the unipolar signal, and part of the loss (3 dB) is due to the factor of 2 smaller peak-to-peak signal power for unipolar signals compared to bipolar signals.

Note that for all of the configurations discussed, the use of only a single channel of mixing between the LO and signal can result in up to a 3 dB loss in electrical power SNR compared to summing the outputs of in-phase and quadrature phase LO and signal mixing channels (i.e., compared to using I-Q detection) (Minkoff,1992).

For the post-detection mixing configuration with a single channel of signal and LO balanced mixing, the theoretical expression for the electrical *current* SNR (which is the square root of the electrical *power* SNR) when the receiver is signal plus background shot noise limited for Poisson distributed photon arrival intervals is

$$SNR = \frac{C_{tot} - C_{bg}}{\sqrt{4 \cdot C_{tot}}} = \frac{C_{sig}}{2 \cdot \sqrt{C_{tot}}}, \qquad (3)$$

where C_{tot} = Total Number of Counts in the Measurement

C_{bg} = Total Number of Background Counts in the Measurement

C_{sig} = C_{tot} - C_{bg} = Total Number of Signal Counts Measured

where the factor of 4 under the radical in the denominator is due to a factor of 2 (3dB) loss in electrical power SNR due to the one-sided nature of the signal modulation, and a factor of 2 (3 dB) loss in electrical power SNR due to not employing I-Q detection as discussed above.

For the OEM configuration with a single channel of signal and LO mixing, the theoretical expression for the electrical *current* SNR when the receiver is signal plus background shot noise limited for Poisson distributed photon arrival intervals is

$$SNR = \frac{C_{tot} - C_{bg}}{\sqrt{16 \cdot C_{tot}}} = \frac{C_{sig}}{4 \cdot \sqrt{C_{tot}}}, \qquad (4)$$

where the additional factor of 4 (6 dB) reduction in electrical *power* SNR compared to the post-detection mixing configuration is due to the unipolar mixing process inherent in the gated OEM configuration (Wozencraft, 1965).

3. SIMULATION RESULTS

3.1 Computer Simulation

We developed a computer simulation of the photon counting chirped AM ladar technique in MathCAD[TM]. Here we present results from the computer simulation

using a *two-sided (bipolar)*, sinusoidal chirp LO and a signal consisting of *one-sided (unipolar)*, Poisson distributed pulses with square wave chirp-modulated mean arrival rates. This configuration corresponds to the post-detection mixing configuration discussed above. Figure 5 shows the IF waveform, and Figure 6 shows the magnitude spectrum of this IF waveform from this simulation for a chirp bandwidth of 100 MHz (10 MHz to 110 MHz chirp), a chirp duration of 0.53 ms (limited by computer resources), an IF frequency of 20.77 kHz, 1990 signal counts, and zero background counts. As expected, there is a peak in the magnitude spectrum at the IF frequency of 20.77 kHz. The theoretically calculated electrical *current* SNR for the simulation parameters is 22.3, and the measured SNR for this simulation is 23.2, yielding a difference between simulation and theory of 4%.
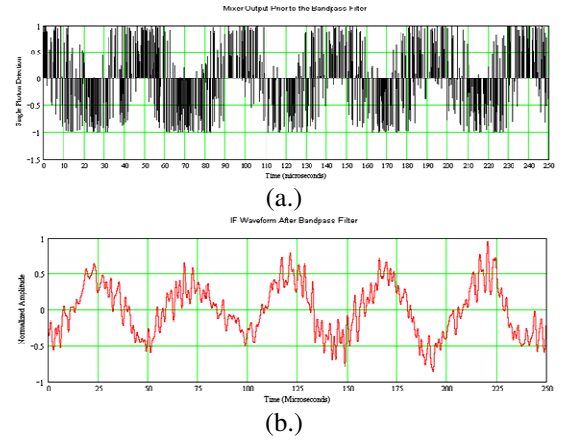

(a.)

(b.)

Figure 5. IF waveform from the Computer Simulation (a.) prior to bandpass filtering, and (b.) after bandpass filtering
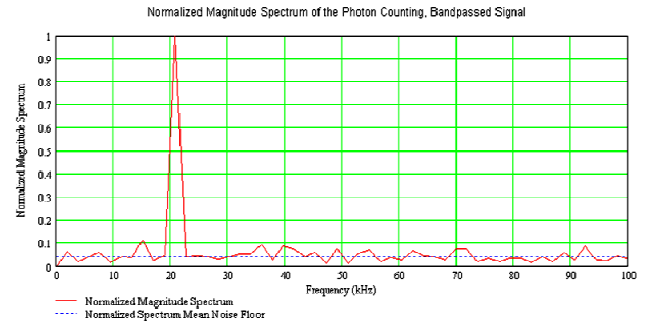

Figure 6. Normalized Magnitude Spectrum of an IF Waveform from the Computer Simulation

3.2 Electronic Hardware Simulation

A block diagram of the electronic hardware simulation setup is shown in Figure 7. This electronic simulation setup produces a *two-sided (bipolar)*, sinusoidal chirp LO mixed with a signal consisting of *one-sided (unipolar)*, Poisson distributed, 2 ns wide pulses with square wave chirp-modulated mean arrival rates. This

corresponds to the post-detection mixing configuration with a sinusoidal LO and a square wave signal modulation. A LabView™ virtual instrument program loads an array of 1's and 0's into the on-board buffer memory of a digital input/output (DIO) card in a personal computer (PC). The 1's and 0's are Poisson distributed. A manually initiated signal generator (signal generator 1 in the block diagram) outputs a pulse which triggers a pulse generator that acts as the clock for the DIO card, and triggers the enable lines on the DIO card to start outputting the digital pulses in synchrony with the clock pulses. Ones correspond to signal pulses and zeros to the absence of signal pulses.
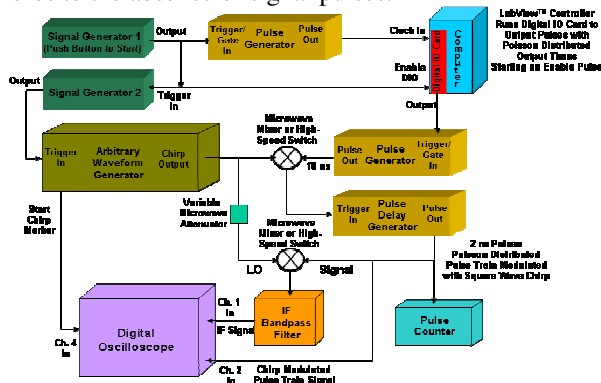

Figure 7. Block diagram for the electronic simulation.

The output pulse from signal generator 1 also triggers the start of signal generator 2, which operates in burst mode to output trigger pulses to the arbitrary waveform generator's (AWG's) trigger input. The AWG outputs the sinusoidal chirp signal with the chirp implemented as discrete frequency steps, with the frequency stepping up on each input trigger pulse. The chirp waveform output by the AWG is split into two paths: on one path the chirp waveform is input to a microwave mixer that mixes the chirp signal with a train of 10 ns pulses output by a pulse generator that is edge triggered by the longer pulses output by the DIO card; on the other path the chirp waveform is sent through a variable microwave attenuator to a microwave mixer as the LO signal.

The output of the mixer in the first path is a two-sided, sinusoidally modulated train of pulses. This signal is input to the trigger input of another pulse generator. The trigger input of this pulse generator is set up as a rising edge trigger with a positive threshold, thereby eliminating the negative going pulses. This pulse generator also has a variable delay to simulate round-trip propagation delays. The output of this pulse generator is a train of equal amplitude, one-sided, 2 ns duration, Poisson distributed pulses with a square wave chirp arrival rate modulation that represents the received signal for a photon counting chirped AM ladar for which the transmitter chirp waveform is a square wave. This signal is sent to the RF signal input of the same microwave mixer to which the chirped LO signal (from the second

of the two paths described above) is sent. The variable microwave attenuator on the LO signal path is set to prevent the LO from saturating the mixer. The output of this mixer is sent through an IF bandpass filter to channel 1 of the digital oscilloscope. Part of the signal before the mixer is split into two other signal paths, with one input to a pulse counter and the other input to channel 2 of the digital oscilloscope. The pulse counter measures the number of pulses (representing photo-counts) in the signal. Channel 2 of the digital oscilloscope is just used to monitor the output of the pulse generator to determine when the trigger threshold is set properly. Channel 4 of the digital oscilloscope receives a marker pulse from the chirp generator indicating the start of the chirp, and the oscilloscope is triggered on this channel so that the data collection is synchronized with the chirp.

The IF signal output of the mixer and bandpass filter that is input to channel 1 of the digital oscilloscope is digitized and displayed by the digital oscilloscope. In addition, the digital oscilloscope computes the magnitude spectrum of the IF signal. Both the raw IF signal digital data and the computed magnitude spectrum digital data are saved to disk by the oscilloscope. This data is then transferred to a PC for processing and plotting.

Figure 8 shows the normalized magnitude spectrum of an IF waveform from this electronic simulation for a chirp bandwidth of 100 MHz, a chirp duration of 4.2 ms, an IF frequency of 2 kHz, and 2024 signal counts. Theoretically, the electrical *current* SNR for these parameters is 22.5 for this setup. For this simulation, the theoretical SNR differs by only 0.9% from the measured SNR of 22.3.
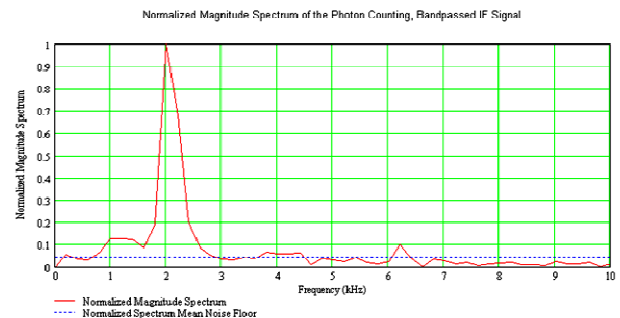

Figure 8. Normalized Magnitude Spectrum of an IF Waveform from the Electronic Hardware Simulation.

4. EXPERIMENTS

4.1 Experimental Setup

We set up a proof-of-principle (PoP) laboratory optical experiment with a Perkin-Elmer, fiber pigtailed silicon SLIK™ Gm-APD SPCM (60% photon detection efficiency at 785 nm wavelength) and a ~ 785 nm wavelength, fiber pigtailed diode laser. The top-level

layout of this initial proof-of-principle laboratory optical experiment is shown in Figure 9. The experimental layout is very similar to that of the photon counting chirped AM ladar in the post-detection mixing configuration shown in Figure 3, except that the generic laser shown in Figure 3 is replaced with a fiber pigtailed diode laser, only one chirp generator is used in the laboratory setup, and the free-space round-trip path between the ladar transceiver and the target is replaced with an all optical fiber path through several variable optical attenuators (VOAs).
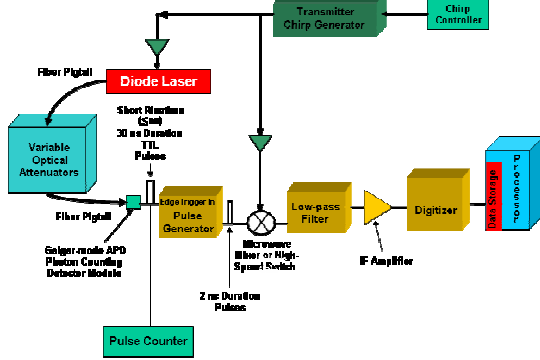

Figure 9. Top-level layout for the laboratory proof-of-principle optical experiment.

Different ranges are simulated by varying the delay between the trigger input and the pulse output on the pulse generator. The VOAs are used first to attenuate the laser output by at least 100 dB to prevent damage and/or saturation of the photon counting detector module, and second to vary the number of received photo-counts from a few hundred to a few thousand to verify the predicted scaling of the SNR for the IF signal's magnitude spectrum. Four fiber-based VOAs plus four fixed optical attenuators are used to provide the very large, controllable optical attenuations needed.

In the initial experimental setup, the shortest duration pulse capable of being output by the pulse generator was 2 ns (full width at half maximum (FWHM)), which limited the highest useful chirp frequency to about 125 MHz in the initial setup. Subsequently, we replaced the first pulse generator with one that output 0.6 ns pulses, limiting the highest useful chirp frequency to 416 MHz.

To implement the OEM configuration, the short pulse generator and the microwave mixer were removed, and the sinusoidal chirped LO was converted to a 5 V square wave that gates the input of the Perkin-Elmer SPCM.

4.2 Post-Detection Mixing Results

Figure 10 shows the magnitude spectrum of the IF waveform from the first chirped AM optical experiment using the setup as depicted in Figure 9. The following parameters were used for the experimental results shown

in Figure 10: Chirp duration: 20 s over a total chirp bandwidth of 200 MHz (from 10 MHz to 210 MHz), Chirp BW over the 1.024 second measurement duration: 10.24 MHz, IF: 92.77 Hz, IF Filter Upper Freq: 100 Hz, IF Filter Lower Freq: 10 Hz, Sampling Rate: 1 KSamples/s, Measurement Duration: 1.024 s, Number of Samples: 1024, Background Counts (Dark Counts + Ambient Light Counts) for the Measurement: 245 counts, and Total Counts for the Measurement: 800 counts. In the setup for this experiment the start of the chirp and the start of data collection were not synchronized so a much longer chirp duration than measurement duration was set on the chirp generator so that the measurement could be made without crossing the transition from the end of one chirp to the beginning of the next chirp. This resulted in a much smaller chirp bandwidth (10.24 MHz) for the measurement than the chirp generator output's full bandwidth (200 MHz).
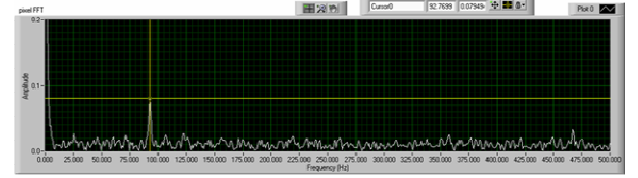

Figure 10. Magnitude spectrum of the IF waveform from the first chirped AM ladar with a photon counting receiver proof-of-principle laboratory optical experiment.

The measured electrical *current* SNR for these results is 7.9, which is 19.4% lower than the calculated SNR of 9.8 for the given signal and background counts. The electrical *power* SNR measured for the Gm-APD receiver in this experiment was within 3.5 dB of the theoretical signal shot noise limit ($C_{sig}/4$) for the chirped AM waveform used, and within 1.9 dB of the theoretical limit determined by both the signal shot noise and the shot noise due to the measured background counts. Since the photon detection efficiency of the photon counting module is about 60% at 785 nm, the number of signal photons required to achieve the SNR of 7.9 in the experiment is (800-245)/0.6 = 555/0.6 = 925 photons.

If we model the loss in SNR between the theoretical value predicted by equation (3.) and the experimentally measured value as due to some unknown, equivalent additive number of excess noise counts (due to, for example, noise in subsequent electronics such as the IF filter amplifier, less than unity mixing efficiency, chirp nonlinearity, and/or incomplete modulation of the laser), we can calculate the equivalent number of excess noise counts from the following equations:

$$SNR_{meas} = \frac{C_{tot} - C_{bg}}{\sqrt{4 \cdot (C_{tot} + C_{excess})}} = \frac{C_{sig}}{\sqrt{4 \cdot (C_{sig} + C_{bg} + C_{excess})}} \quad (5\text{ a})$$

and, therefore,

$$C_{excess} = \frac{1}{4} \cdot \left(\frac{C_{sig}}{SNR_{meas}}\right)^2 - \left(C_{sig} + C_{bg}\right) \quad (5\text{ b})$$

where   SNR$_{meas}$ = the measured electrical
current signal-to-noise ratio
C$_{excess}$ = the equivalent excess noise
counts causing the SNR
degradation from the
theoretical SNR.

For the experiment with SNR$_{meas}$ = 7.9, C$_{sig}$ = 555 counts, and C$_{bg}$ = 245 counts, we calculate C$_{excess}$ from equation (5 b.) to be 434 counts.

By setting the SNR = 1 and solving for C$_{sig}$ in equation (3), we find the following equation for the theoretical Noise Equivalent Photocounts in the absence of excess noise counts:

$$C_{sig\_NEP} = 2 \cdot \left[1 + \sqrt{1 + C_{bg}}\right] \qquad (6)$$

This reduces to C$_{sig\_NEP}$ = 4 in the absence of background counts, as it should for the signal shot noise limited case for which SNR = (C$_{sig}$/4)$^{1/2}$. Thus, for the signal shot noise limited case in the absence of background and excess noise counts, the noise equivalent photon (NEPh) sensitivity for 60% photon detection efficiency is 4/0.6 = 7 photons. For C$_{bg}$ = 245 counts, as in the experimental results presented here, C$_{sig\_NEP}$ = 33.369. Thus, with a photon detection efficiency of 60% and a background count of 245 counts, the theoretical NEPh sensitivity is 56 photons in the absence of any excess noise counts.

By setting the SNR$_{meas}$ = 1 and solving for C$_{sig}$ in equation (5 a), we find the following equation for the Noise Equivalent Photocounts for the experimental setup including the excess noise counts:

$$C_{sig\_NEP\_meas} = 2 \cdot \left[1 + \sqrt{1 + C_{bg} + C_{excess}}\right] \qquad (7)$$

For C$_{bg}$ = 245 counts and C$_{excess}$ = 434 counts, as for the experimental results presented here, C$_{sig\_NEP\_meas}$ = 54.1536. Thus, with a photon detection efficiency of 60%, a background count of 245 counts, and an excess noise count of 434 counts, the NEPh sensitivity for the experimental setup is 54.1536/0.6 = 90 photons. Since estimates of the NEPh sensitivity of the existing unity gain solid state detector-based chirped AM ladar breadboard is about a million photons, these experimental results indicate an improvement in sensitivity by about four orders-of-magnitude.

After upgrading the experimental setup with a pulse generator outputting 0.6 ns pulses, we ran the experiment again, but with the following parameters: Chirp: 20 MHz – 320 MHz for 1 second duration; IF: 248 Hz, IF Sampling Rate: 5 kHz, Number of Samples: 5000, IF Bandpass Filter: 100 Hz - 300 Hz, Signal Counts: 785 counts; Background Counts: 115 counts. Figure 11 shows the power spectrum resulting from this experiment. The measured electrical *power* SNR for this data is 22.15 dB, which is only 0.18 dB less than the

theoretical SNR of 22.33 dB. Equations (5 b) and (7) yield an excess noise counts value of 40.3 and an NEPh sensitivity of 45 photons for this experiment.
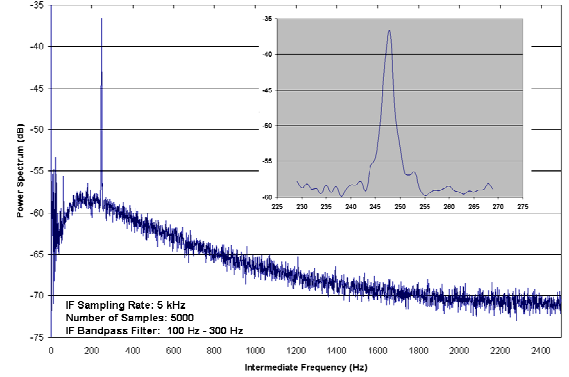

Figure 11. Power Spectrum of the IF Waveform for the experiment with a 0.6 ns pulse generator and a 300 MHz chirp bandwidth.

4.3 Opto-Electronic Mixing (OEM) Results

In order to test the OEM configuration shown in Figure 4, we modified the laboratory setup shown in Figure 9 by removing the sub-nanosecond pulse generator and microwave mixer. We then input the sinusoidal LO signal into the trigger input of a pulse/signal generator to produce a chirped square wave of 0 to 5 V amplitude. This square wave LO was applied to the gate input of the Perkin-Elmer SPCM. Since the minimum gate duration for the Perkin-Elmer SPCM is 50 ns, the maximum chirp frequency that can be used in this setup is about 10 MHz. Most of the microwave components in the setup have a frequency response that starts to roll off below 10 MHz. Thus, the useful chirp bandwidth is very limited for this setup in the OEM configuration. For the experiment, we chirped from 9 MHz to 10.49 MHz for a chirp bandwidth of 1.49 MHz, over a 1.024 second duration. In order to get sufficient delay time, we used a chirp generator with two direct digital synthesizers (DDS's), one for the signal and one for the LO, so that the we could program a desired delay between the signal and LO chirps. For this experiment, the delay was set at 100 μs. The power spectrum of the IF waveform for this experiment, accumulated over 5 seconds at a 1 kS/s sampling rate, is shown in Figure 12. Based on the chirp bandwidth, chirp duration, and delay time, the predicted frequency of the peak in the IF spectrum is 145.5 Hz. For this experiment, the number of signal counts is 265000, and the number of background counts is 700. The predicted electrical *power* SNR for these parameters is 42.18 dB, and the measured electrical *power* SNR for the results shown in Figure 12 is 36.42 dB, which differs from the theoretical prediction by -5.76 dB. This corresponds to a factor of almost 4 times lower electrical *power* SNR and almost 2 times lower electrical *current* SNR than theoretically predicted. The source of SNR loss in this experiment is

currently unknown, but may be due to incomplete modulation of the laser, excess noise caused by gating the SPCM at high frequencies, excess noise from the IF amplifier, excess noise during the "flyback" time between chirps, and/or peak spreading due to anomalies in the chirp (nonlinearities, timing jitter, etc.).
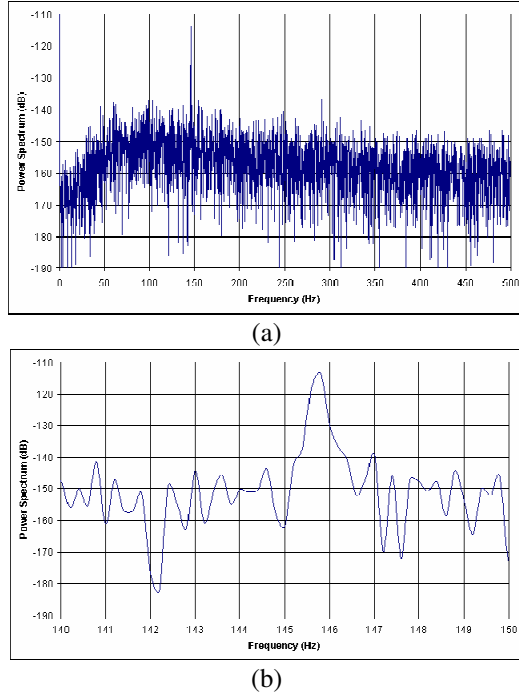

(a)

(b)

Figure 12. Power Spectrum of the IF waveform for the experiment in the OEM configuration (a) over a 500 Hz IF bandwidth, and (b) "zoomed" from 140 Hz to 150 Hz.

CONCLUSIONS

The simulation and experimental results presented here demonstrate the viability of the photon counting chirped AM ladar technique, and verify the theory of operation and theoretical SNR calculations. For the first proof-of-principle laboratory optical experiment with a 10.24 MHz chirp bandwidth reported in section 4.2, we achieved an SNR of 7.9 with 925 signal photons, corresponding to an NEPh sensitivity of 90 photons in the presence of 245 background counts and 434 excess noise counts with a photon detection efficiency of 0.6. After upgrading the experimental setup with a sub-nanosecond pulse generator, we demonstrated an electrical *current* SNR of 12.8, compared to a theoretical SNR of 13.08 for this experiment with 785 signal counts, 115 background counts, and a 300 MHz chirp bandwidth. For this experiment, the measured SNR differs from the theoretical SNR by only 2.14%, and corresponds to an NEPh sensitivity of 45 photons. We demonstrated operation in both the post-detection mixing and the opto-electronic mixing configurations.

Estimates of the NEPh sensitivity of a chirped AM ladar operating with unity gain, linear response mode, metal-semiconductor-metal (MSM), optoelectronic mixing (OEM) detectors are on the order of a million photons per pixel. The experimental results presented here indicate an NEPh sensitivity of the single pixel chirped AM ladar with a photon counting receiver of under one hundred photons. This represents an improvement in sensitivity by a factor of more than 10^4. This sensitivity improvement assumes that measures are taken to restrict the background and excess noise counts to the levels achieved in the experiments.

ARL's chirped AM ladar technique using photon counting detectors requires relatively low readout bandwidths and low digital sampling rates after the mixer because the mixing process downconverts the signal to the low frequencies of the IF band (usually less than MHz) without loss of the range resolution provided by the wide bandwidth chirp waveform (usually in the hundreds of MHz to GHz regime).

The 10^4 sensitivity improvement demonstrated by the photon counting chirped AM ladar experiments may enable very compact, low power, eye-safe, and/or long range ladars with low cost, low bandwidth readout integrated circuits.

ACKNOWLEDGMENTS

REFERENCES

Drain, L.E., *The Laser Doppler Technique*, New York: John Wiley & Sons (JW&S), 1980, pp. 145-147.

Minkoff, John, Signals, Noise, and Active Sensors: Radar, Sonar, Laser Radar, New York: JW&S, 1992, pp. 118-129 and 144-146.

Stann, B.L., W.C. Ruff, and Z.G. Sztankay, "Intensity-modulated diode laser radar using frequency modulation/continuous-wave ranging techniques," *Optical Engineering,* Vol. 35, No. 11, 1996, pp. 3270-3278.

Wozencraft, John M., and Irwin Mark Jacobs, Principles of Communication Engineering, New York: JW&S, 1965, p.639.